Utilization of composite adsorbents for polycyclic aromatic hydrocarbons adsorption from vehicle wash wastewater and aqueous solutions

Muhammad Ilyas[a,*], Waqas Ahmad[b], Hizbullah Khan[a]

[a]*Department of Environmental Sciences, University of Peshawar, Peshawar, Khyber Pakhtunkhwa, Pakistan, Tel. +923078064028;
emails: sirfilyas@yahoo.com (M. Ilyas), hizbullah@uop.edu.pk (H. Khan)*
[b]*Institute of Chemical Sciences, University of Peshawar, Peshawar, Khyber Pakhtunkhwa, Pakistan, email: waqasahmad@uop.edu.pk*

ABSTRACT

This study aims to remove polycyclic aromatic hydrocarbons (PAHs) from both vehicle wash wastewater and aqueous solutions through batch experiment utilizing composite adsorbents. The composite adsorbents such as waste polystyrene/biochar/bentonite (wPS/C/Bt) and waste polyethylene terephthalate/biochar/bentonite (wPET/C/Bt) were prepared using waste polystyrene (wPS) and waste polyethylene terephthalate (wPET) as matrix and bentonite clay and biochar as filler. The synthesized wPS/C/Bt and wPET/C/Bt were used as adsorbents for the adsorption of PAHs from vehicle wash wastewater as well as aqueous solution. The prepared composite adsorbents were investigated by Fourier-transform infrared spectroscopy, surface area analyser, as well as scanning electron microscopy. To study the PAHs adsorption by wPS/C/Bt and wPET/C/Bt, the batch adsorption process was performed with different factors such as temperature, contact time, pH, initial PAHs concentration and the dose of adsorbents. The equilibrium isotherms were tested by Langmuir and Freundlich models. In addition, the adsorption kinetics were explored using pseudo-second-order as well as pseudo-first-order models. The acquired adsorption kinetic statistics show that the process fits the Langmuir and pseudo-second-order model. The various thermodynamic factors, like Gibbs free energy ($\Delta G°$), enthalpy ($\Delta H°$) and entropy ($\Delta S°$) have shown that the process of adsorption PAHs onto wPS/C/Bt and wPET/C/Bt was an endothermic and non-spontaneous process. The results of this study show that wPS/C/Bt and wPET/C/Bt exhibit higher efficiencies (>70%) and can be used as promising adsorbents while eliminating PAHs from wastewater.

Keywords: Waste polystyrene; Waste polyethylene terephthalate; Biochar; Bentonite; Vehicle wash wastewater; Aqueous solution; Polycyclic aromatic hydrocarbons; Adsorptive removal

1. Introduction

The United States Environmental Protection Agency (USEPA) priority pollutants list includes the 16 polycyclic aromatic hydrocarbons (PAHs); fluoranthene (Flu), benz(a)anthracene (BaA), phenanthrene (Ph), acenaphthene (Ace), benzo(ghi)perylene (B[ghi]P), dibenz(a,h)anthracene (D[ah]A), indeno(1,2,3-cd)pyrene (InP), benzo(a)pyrene (BaP), benzo(b)fluoranthene (BbF), benzo(k)fluoranthene (BkF), acenaphthylene (Acy), fluorene (Fl), naphthalene (Nap), anthracene (Ant), pyrene (Pyr), and chrysene (Chr) [1].

PAHs are organic compounds composed of two or more fused aromatic rings bonded in clustered (e.g., Pyr), angular (e.g., D[ah]A or linear (e.g., Ant) arrangements [2]. These compounds persist in the environment and have adverse effects on health. These characteristics make it an essential category of environmental pollutants [3]. Due to the presence of at least two aromatic rings, they have low water solubility, low volatility, as well as a stable hydrophobic planar configuration [4]. The source of PAHs is both man-made and natural. Open burning, coal deposits or oil emissions or natural losses, forest and bush fires,

* Corresponding author.

and volcanoes are natural sources of PAHs [5,6]. The PAHs anthropogenic sources form through catalytic cracking, high temperature cooking (e.g., frying, grilling, in addition to charbroiling), tobacco smoking, petroleum refining, production of asphalt, coke, and aluminum, coal gasification, car exhaustion and residential heating [2,3].

PAHs are used in wood preserving, plastics, dyes, resins, pesticides, manufacturing of pigments, lubricating materials, agricultural products, and pharmaceuticals [2]. Leakage or spillage of oil, urban surface runoff, industrial effluents, municipal litters, and atmospheric fallout are the means that release PAHs into natural water resources [6]. PAHs are observed mostly in the surface soil due to surface runoff or atmospheric deposition. Coal-tar linings of the distribution pipes are the major source of PAHs in drinking water [3]. The main way for the public to be exposed to PAHs is through ambient and indoor air and food intake. Skin absorption and inhalation are occupational exposures to PAHs [3].

PAHs can cause long-term and temporary health effects. In humans, the temporary health effects are unclear. Although, confusion, diarrhea, vomiting, nausea, and eye irritation are temporary health effects of occupational exposure to high levels of PAHs [2]. High volatility is a characteristic of low molecular weight PAHs (such as Nap), which brings short-term hazards through inward breathing without causing malignant tumors [7]. Long-term introduction of PAHs can cause health effects, including lung system abnormalities, asthma symptoms, difficulty inhaling, liver and kidney damage, cataracts, and immune system suppression [2]. PAHs with elevated sub-atomic weight (e.g., BaP) are distinguished as individual cancer-causing agents and can release into nature [8]. Due to the persistence of PAHs in nature, it will cause them to accumulate in food, soil, water, and air. After entering the human body, PAHs can basically pass through the cell layer and successfully adsorb into the cells. Therefore, the immune system converts PAHs into epoxide hydrolase and diepoxide, which react with DNA and prevent its production [9,10].

PAHs have an unfavorable wellbeing impact on aquatic as well as human health; in this way, they should be eliminated from environmental media. Various strategies have been examined to eliminate PAHs from polluted waters as well as soils to mitigate the possible harm of PAHs to human wellbeing and the environment. Chemical, thermal, biological, phytoremediation, as well as physical processes (which comprise incineration, thermal desorption, radio frequency heating, oxidation, ion exchange, photolysis, adsorption, electrolysis, chemical precipitation, natural attenuation, biostimulation, bioaugmentation, rhizofiltration, phytoextraction, phytostabilisation, and phytoremediation) are the most significant treatment strategies of PAHs contaminated waters, soil as well as sediments [11–16].

The adsorption strategy is simple in design, easy to operate, insensitive to toxic pollutants, and low in cost. Therefore, it is a powerful technology to remove PAHs from aqueous media. The elimination efficiency of the adsorption method can reach 99.9% [17]. In this way, people are increasingly keen to find reasonable adsorbents to eliminate these toxins from water. During the adsorption process, pollutants will accumulate on the interface or surface of the adsorbent. In the water treatment process, the adsorption process occurs at the interface between the sewage and the solid adsorbent. The adsorption phase and the adsorbed pollutants are called adsorbent and adsorbate, respectively [17]. Various adsorbents used for this purpose include hen feather [18], ZnNiIn layered double hydroxides derived mixed metal oxides [19], Fe-benzene dicarboxylic acid metal organic framework [20], various adsorbents for caffeine, nicotine and amoxicillin [22], Waste material a non-carbon adsorbent nano alumina [22], iron-based metal organic framework [23], waste rubber tires [24], chitosan grafted polyaniline [25], papaya peel carbon [26], iron oxide-impregnated dextrin nanocomposite [27], green synthesis of silver nanoparticles [28], montmorillonite clay [29], poly (methyl methacrylate)-grafted alginate/Fe$_3$O$_4$ nanocomposite [30], L-cysteine-modified montmorillonite-immobilized alginate nanocomposite [31], waste polystyrene/biochar/bentonite (wPS/C/Bt) and waste polyethylene terephthalate/biochar/bentonite (wPET/C/Bt) [32,33], activated carbon [34,35]. The basic objective of this study is to use wPET/C/Bt as well as wPS/C/Bt to remove PAHs from vehicle wash wastewater and aqueous solution. Due to the use of alternative sources such as wPS and wPET, the process of preparing composite adsorbents is a relatively effective and low-cost method. In addition, various test conditions were set to determine their effects and explore the ideal removal performance of composite adsorbents.

2. Experimental

2.1. Sample collection and preparation

Standard solutions of PAHs Mix-13 (USEPA 16) consisting of benz(a)anthracene (BaA; 10 µg/L), benzo(a)pyrene (BaP; 10 µg/L), benzo(k)fluoranthene (BkF; 10 µg/L), benzo(b)fluoranthene (BbF; 10 µg/L), dibenz(a,h)anthracene (D[ah]A; 10 µg/L), benzo(ghi)perylene (B[ghi]P; 10 µg/L), indeno(1,2,3-cd)pyrene (InP; 10 µg/L), pyrene (Pyr; 10 µg/L), chrysene (Chr; 10 µg/L), fluoranthene (Flu; 10 µg/L), acenaphthene (Ace; 10 µg/L), acenaphthylene (Acy; 100 µg/L), anthracene (Ant; 10 µg/L), phenanthrene (Ph; 10 µg/L), fluorene (Fl; 10 µg/L) and naphthalene (Nap; 100 µg/L) purity >99% was purchased from Supelco Company, USA. On daily basis, the working standard solution were prepared by diluting the PAHs Mix-13 standard solution in 2-propanol. Thus, as to avert photochemical degradation, the sample extracts and standard solutions were stored in brown glass vials for further study at 4°C [34]. The vehicle wash wastewater samples from both heavy vehicle-wash stations and light vehicle-wash stations were collected using the same protocol as given in our previous articles [32,34].

2.2. Synthesis of composite adsorbents from waste plastics

The composite materials were synthesized by incorporating bentonite clay and biochar as fillers into wPS and wPET polymer matrix, in different percentage ratios. In a typical procedure, known amount of wPS and wPET was dissolved in acetone and different amounts of bentonite clay and biochar was suspended in it by sonication at 35°C temperature for 1 h. The slurry was poured into petri dish

and placed in vacuum oven to remove the solvent. The solid mass was ground into fine powder and stored in glass vials for further study.

2.3. Characterization of composite adsorbents

The adsorbent prepared in the laboratory were characterized by relevant instrumental analysis, including scanning electron microscopy (SEM; JSM-5910, JEOL, Japan), Fourier-transform infrared spectroscopy (FTIR; Spectrum Two, S. No: 103385) analysis, and surface area analysis (NOVA 2200e, Quantachrome, USA), in order to study the surface morphology, functional groups, and surface area, respectively.

2.4. Adsorption experiments

The batch adsorption tests were carried out for the adsorption of PAHs from vehicle wash wastewater and aqueous solution by wPS/C/Bt and wPET/C/Bt. At 24°C ± 2°C, put about 100 mL of sample containing PAHs into a 500 mL Erlenmeyer flask, add a certain amount of wPS/C/Bt and wPET/C/Bt to it, and stir at 150 rpm on a magnetic stirrer until it reaches equilibrium. In the study, various variables were measured, including pH of the solution (3, 5, 6, 9, and 11), PAHs concentrations (10, 20, 30, and 40 ppm), contact time (0.25, 0.5, 1 and 1.5 h), and dose of adsorbent (0.2, 0.4, 0.6, and 0.8 g/100 mL), pH was adjusted by adding NaOH to the solution as needed. For all tests carried out, the mean values of triplicate were presented.

2.5. Analyses and calculations

Use UV-Vis spectrophotometry (Shimadzu UV-1700, Japan) to detect the concentration of PAHs in the processed samples of vehicle wash wastewater and aqueous solution [36]. The percentage adsorption of PAHs and the adsorption efficiency q_e (mg/g) are estimated from the equations as given in Table 1 [32–35].

The adsorption behavior was further studied by applying different adsorption models, namely, Freundlich as well as Langmuir isotherms (Table 2). The adsorption kinetics was also studied by applying the adsorption data to the first and second-order kinetic equations (Table 2). The

Table 1
Equations used for q_e and % q_e calculations

	Equation	
Equilibrium concentration	$q_e = \dfrac{\left[(C_o - C_i) \times V\right]}{M}$	(1)
	where,	
	C_o (µg/L) = initial PAHs concentration;	
	C_i (µg/L) = equilibrium PAHs concentration;	
	V (L) = volume of solution;	
	M (g) = mass of adsorbent.	
Percentage removal	$\%q_e = \dfrac{\left[(C_o - C_i) \times 100\right]}{C_o}$	(2)

influence of temperature on thermodynamics parameters ($\Delta G°$, $\Delta H°$ and $\Delta S°$) was also analyzed (Table 3) [32–35].

3. Results and discussion

Composite adsorbents such as wPET/C/Bt and wPS/C/Bt have been used to study the adsorption of PAHs from aqueous solutions. The initial batch mode adsorption experiment was performed at 24°C ± 2°C for 1 h, and the ratio of adsorbent to solution was 0.3 g/100 mL. The results are given in Fig. 1. Through adsorption experiments under different conditions, the ideal adsorption factors were further studied.

3.1. Characterization of adsorbents

3.1.1. SEM analysis

The composite adsorbents such as wPS/C/Bt and wPET/C/Bt were described by SEM, FTIR, as well as specific surface area analysis. The SEM micrographs of wPS/C/Bt and wPET/C/Bt are displayed in Fig. 2a and b, respectively. The surface morphology of wPS/C/Bt (Fig. 2a) show the stuffing of biochar and bentonite inside the pores of wPS and finally resulted in uniform microcellular foaming in the composite. On the other hand, the wPET/C/Bt SEM micrographs (Fig. 2b) shows that in the holes of wPET, the biochar and bentonite were embedded and combined tightly. In the surface cracks or pores of wPET, there were many club-shaped crystals, which had a much larger size having 9–10 and 5–6 µm length and diameter, respectively.

3.1.2. FTIR spectra

Fig. 3a–f show FTIR spectra of the waste polymers, fillers and the composite adsorbents. The wPS/C/Bt composite FTIR spectrum is shown in Fig. 3e. The absorption bands were detected at 3,630 cm⁻¹ (O–H, stretch), 2,919 cm⁻¹ (=CH₂, stretching), 1,599 cm⁻¹ (C=C, stretching), 1,493 cm⁻¹ (C=C, stretching), 1,451 cm⁻¹ (CH₂ stretching), 1,013 cm⁻¹ (C–O, stretching), 698 cm⁻¹ (C–H, stretching) and 521 (C–H, stretching) cm⁻¹ [32,37–40]. The FTIR spectrum of the wPET/C/Bt (Fig. 3f) presented the absorption bands in the region at 3,630 cm⁻¹ (O–H, bending vibration), 1,634 cm⁻¹ (H–O–H, bond), 1,013 cm⁻¹ (C–O, bending vibration), 698 cm⁻¹ (C–H, bending vibration) and 521 cm⁻¹ (C–H, bending vibration) [33,37–40]. The new wPS/C/Bt and wPET/C/Bt composite adsorbent had functional groups of both the fillers and waste polymers, and therefore its adsorption efficiency was considered to be better than that of fillers or waste polymers.

3.1.3. Surface area analysis

The surface properties, that is, Barrett–Joyner–Halenda surface area (S_{BJH}), Brunauer–Emmett–Teller surface area (S_{BET}), pore volume and pore radius of the fillers and composite adsorbents were determined using N₂ adsorption isotherms at 77.35 K. The results are given in Table 2. The results of surface analysis (Table 4) indicate that in case of biochar and bentonite the calculated S_{BJH} was found to be 14.10 and 22.37 m²/g, the S_{BET} was 18.37 and 43.27 m²/g,

Table 2
Adsorption models used in the study

Model	Equation	
Kinetic models		
Pseudo-first-order	$\ln(q_e - q_t) = \ln q_e + k_1 t$ where, q_e = equilibrium sorption capacity (µg/g); q_t = sorption capacity (µg/g) at time t (h); k_1 = adsorption rate constant for pseudo-first-order.	(3)
Pseudo-second-order	$\dfrac{t}{q_t} = \dfrac{t}{q_e} + \dfrac{1}{k_2 q_e^2}$ k_2 = adsorption rate constant for pseudo-second-order.	(4)
Equilibrium models		
Freundlich	$\ln q_e = \ln K_f + \dfrac{1}{n}\ln C_e$ $1/n$ = measure of intensity of adsorption; K_f = Freundlich adsorption coefficient; n = Freundlich constant; C_e (µg/L) = equilibrium concentration of adsorbate; q_e: amount of adsorbate adsorbed per unit mass of adsorbent (µg/g).	(5)
Langmuir	$\dfrac{C_e}{q_e} = \dfrac{1}{K Q_{max}} + \dfrac{C_e}{Q_{max}}$ K = Langmuir constant relates the energy of adsorption; q_m = maximum amount of PAHs adsorbed per unit mass of adsorbent (µg/g); q_e = amount of adsorbate per mass unit of adsorbent at equilibrium (µg/g); C_e = equilibrium concentration (µg/L).	(6)

Table 3
Equations used for the thermodynamic parameters calculations

Gibbs free energy	$\Delta G° = -RT \ln K_D$ where R is the ideal gas constant, 8.314 J/K mol; T is the absolute temperature in K; K_D is the equilibrium coefficient of the PAHs adsorption on the adsorbent.	(7)
Enthalpy	$\Delta H° = R\dfrac{T_2 T_1}{T_2 - T_1}\ln\dfrac{k_2}{k_1}$	(8)
Entropy	$\Delta S° = \dfrac{\Delta H° - \Delta G°}{T}$	(9)

with pore radius of 14.90 and 16.62 Å and pore volume of 0.01 and 0.02 cm³/g, respectively. In case of wPS/C/Bt and wPET/C/Bt composite the S_{BJH} was found 55.59 and 50.68 m²/g, the S_{BET} was found 44.95 and 58.53 m²/g, with pore radius of 27.71 and 27.68 Å having pore volume of 0.07 and 0.06 cm³/g, respectively. It is clear from the data that the composite adsorbents possess a high surface area and large pore dimensions than the fillers. Hence, the composite sample hold better adsorption potential compared to the fillers.

3.2. Factors affecting the adsorption process

To study the optimal conditions for the highest adsorption of PAHs, an adsorption experiment was carried out under different conditions of concentration of PAHs, adsorbent dose, temperature, time, and pH.

3.2.1. Effect of adsorbent dosage

Use 100 mL of PAHs solution and different amounts of each composite adsorbent ranging from 0.2 to 0.8 g to investigate the effect of adsorbent dosage. Fig. 4a and b show the adsorption of PAHs under different amounts of wPS/C/Bt and wPET/C/Bt. The results show that as the adsorbent dosage increases, the percent adsorption of PAHs also increases. Generally, these results are related to the presence of more available adsorption sites on the surface of the adsorbent as the dose increases [41].
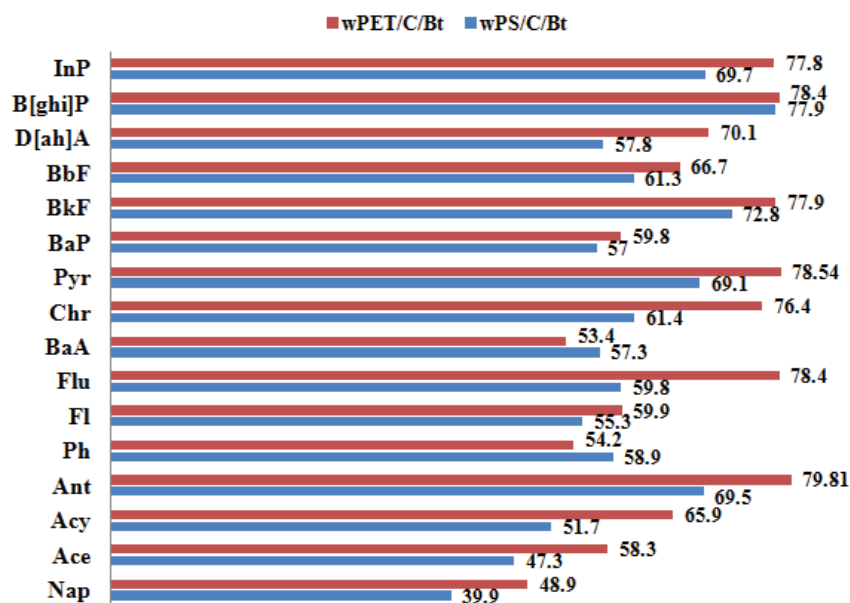
Fig. 1. % adsorption efficiency of composite adsorbents for 16-PAHs from aqueous solution.
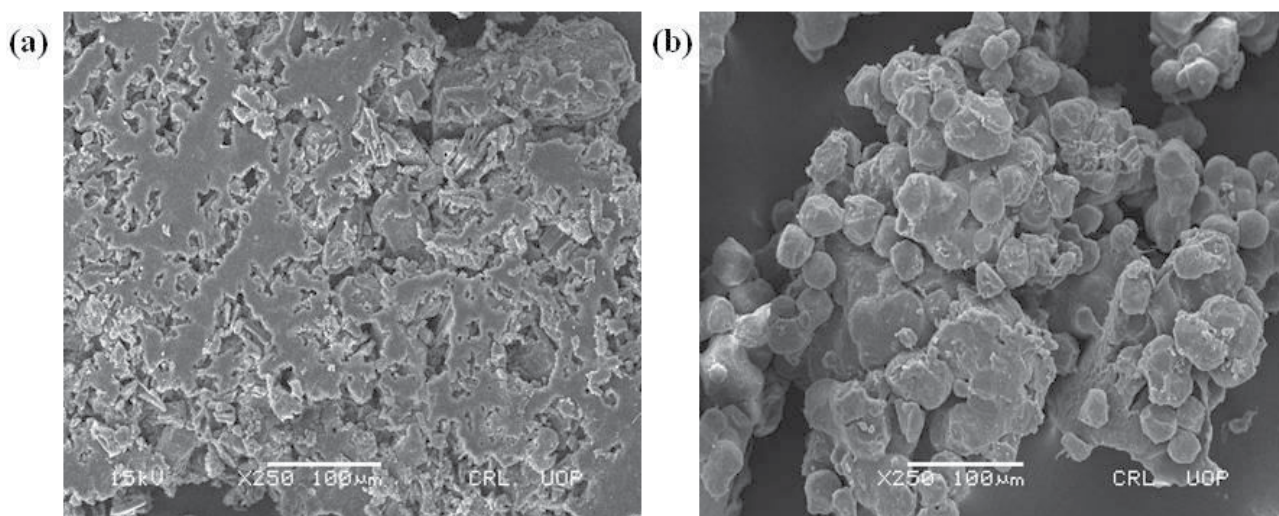

Fig. 2. SEM images of (a) wPS/C/Bt and (b) wPET/C/Bt.

The maximum adsorption percentage of PAHs was achieved at 0.8 g of the adsorbent dosage, which is lower than that reported by [42] and higher than [43]. On the other hand, this value is consistent with [44].

3.2.2. Effect of temperature

Changes in temperature will affect the PAHs adsorption from the wastewater and aqueous solution to the adsorbent. The PAHs adsorption as of aqueous solution by wPS/C/Bt as well as wPET/C/Bt at various temperatures tanning from 20°C to 50°C is shown in Fig. 4c and d, which indicates that the adsorption rate of all PAHs increases with temperature. This also indicates that the PAHs adsorption on the surface of wPS/C/Bt and wPET/C/Bt is endothermic.

The endothermic nature of the adsorption process was reported by many other researchers using various adsorbents, for example, agricultural by-products [45], hen feathers [46], coconut shell activated carbon [47].

3.2.3. Effect of contact time

Through batch adsorption tests with various contact times (i.e., 0.25, 0.5, 1, and 1.5 h), the influence of contact time on the adsorption of PAHs over wPET/C/Bt as well as wPS/C/Bt was investigated. The adsorption of all 16 PAHs over these composite adsorbents increased by up to 1 h, after which it became constant (Fig. 5a and b). This mode may be attributed to the availability of huge number of available active sites on the composite adsorbents surfaces.

After 1 h contact time, most of the active sites available over the composite adsorbents have been occupied and reached equilibrium. Therefore, the optimal contact time is considered 1 h. Similar observations have also been reported in previous studies on the PAHs adsorption over various

Fig. 3. FTIR spectra of (a) biochar, (b) bentonite, (c) wPS, (d) wPET, (e) wPS/C/Bt:1:2:2 and (f) wPET/C/Bt:1:2:2.

adsorbents, that is, the adsorption of PAHs expands as the adsorption time increases and reaches equilibrium [42].

3.2.4. Effect of initial PAHs concentration

The adsorption of PAHs on wPS/C/Bt and wPET/C/Bt was examined under different initial PAHs concentrations. The data is given in Fig. 6a and b, which shows that the percent adsorption of PAHs over both adsorbents increases as the initial PAHs concentration increases from 10 to 40 ppm. This is due to the increase in the initial PAHs concentration which may cause PAHs to be adsorbed on the surface active sites of the adsorbent. Similar behavior was also observed in previous studies, which is due to the effect of the interaction between the adsorbent and the initial PAHs concentration [34,35], it shows that the high initial PAHs concentration has a positive effect, which may be

Table 4
Surface properties of the fillers and composite adsorbents

Adsorbent	S_{BJH} (m²/g)	S_{BET} (m²/g)	Pore radius (Å)	Pore volume (cm³/g)
Biochar	14.10	18.37	14.90	0.01
Bentonite clay	22.37	43.27	16.62	0.02
wPS/C/Bt	55.59	44.95	27.71	0.07
wPET/C/Bt	50.68	58.53	27.68	0.06

Fig. 4. Effect of adsorbent dosage (a, b) and temperature (c, d) on the % adsorption of 16-PAHs over the wPET/C/Bt and wPS/C/Bt.

due to the large amount of PAHs that can interact with the active sites of composite adsorbents.

3.2.5. Effect of pH

The pH value is an essential factor to control PAHs absorption from wastewater as well as aqueous solutions. Using wPS/C/Bt and wPET/C/Bt as adsorbents in the aqueous solution, the effect of pH changes on the PAHs adsorption was investigated, and the study was carried o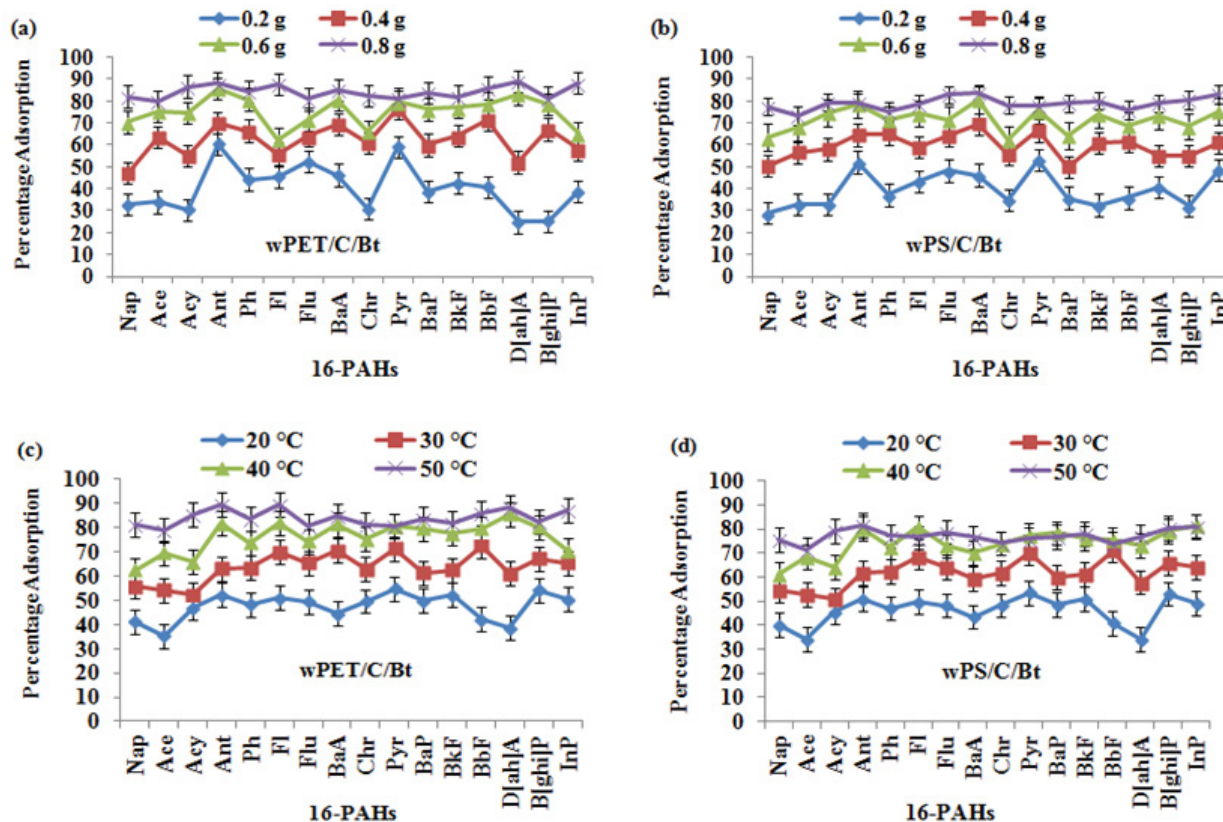ut at different pH values. The % adsorption of PAHs was investigated at different pH, that is, 3, 5, 6, 9, and 11 and the results are given in Fig. 6c and d. Due to the fluctuating adsorption degree of the surface charge distribution of the adsorbent, the adsorption limit is affected by the pH value of the solution, as shown by the functional group of the adsorbate [48]. It can be observed from the data that the % adsorption of PAHs increases with an increase in the pH value of the solution and reached up to maximum adsorption at pH 6. The adsorption capacity of all PAHs in acidic
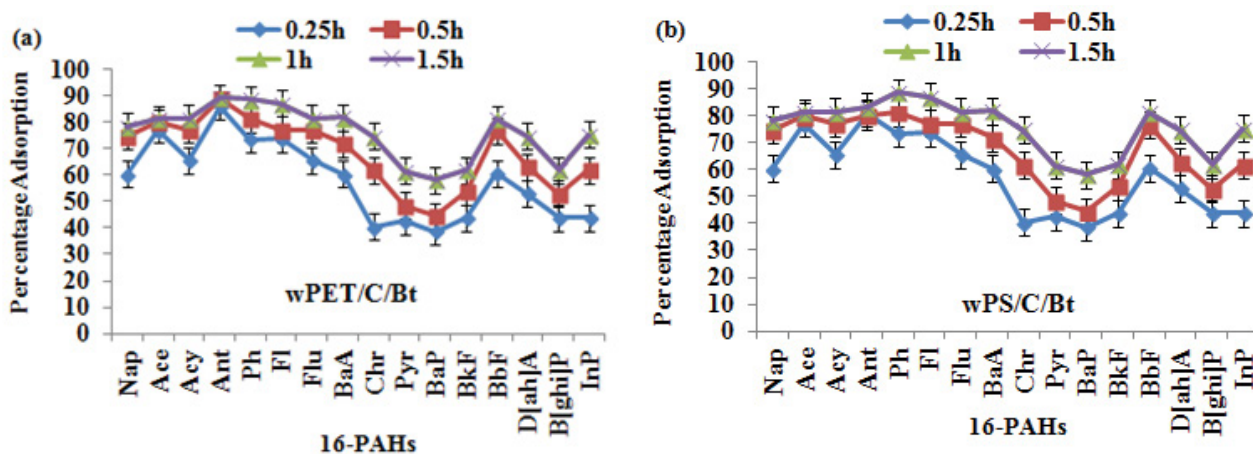

Fig. 5. Effect of contact time (a, b) on the % adsorption of 16-PAHs over the wPET/C/Bt and wPS/C/Bt.
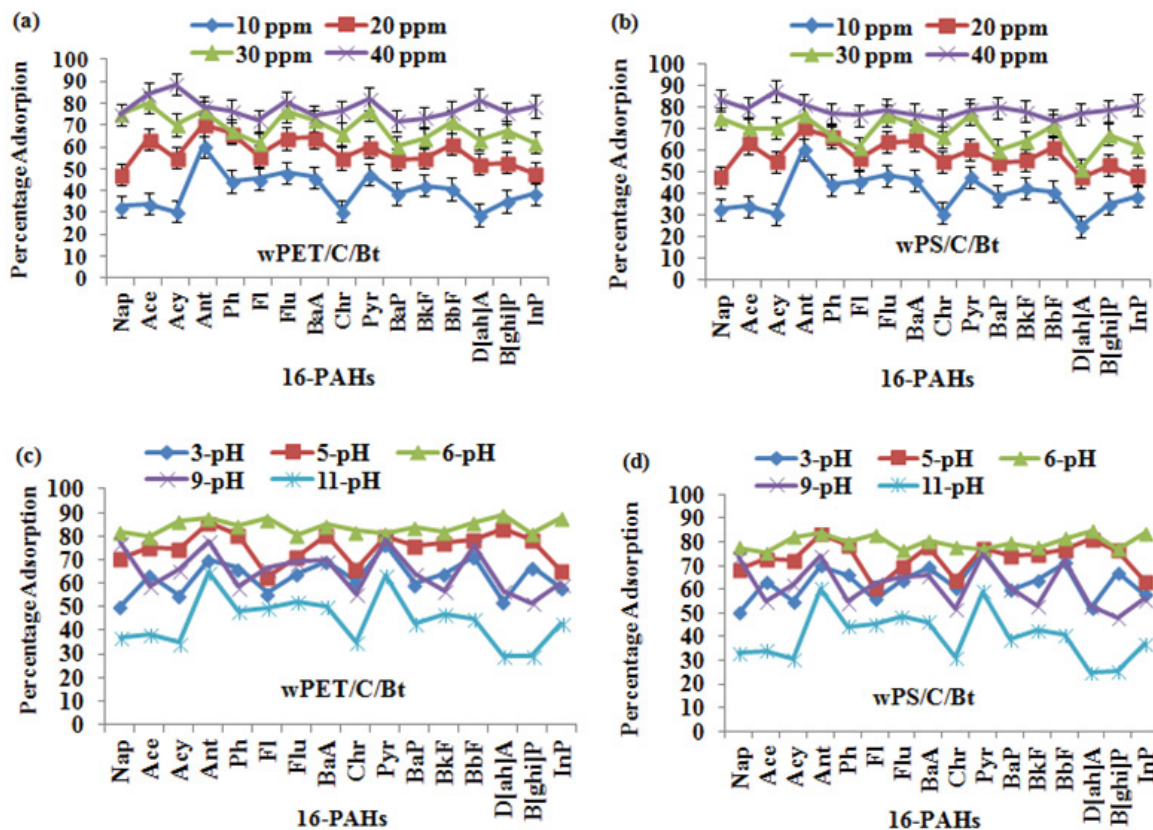

Fig. 6. Effect of initial concentration (a, b) and pH (c, d) on the % adsorption of 16-PAHs over the wPET/C/Bt and wPS/C/Bt.

medium is relatively low, which may be due to the competition between the PAHs and H_3O^+ or H^+ ions found in solution for the same negatively charged sites on the adsorbent [49]. When the pH value of the solution increases from 7 to 11, the adsorption rate gradually decreases due to the electrostatic repulsion of polycyclic aromatic hydrocarbons and composite adsorbents at higher pH values [41].

3.3. Adsorption kinetics

In the batch adsorption experiment, the adsorption behaviour of adsorbents during PAHs adsorption from vehicle wash wastewater was studied by applying the kinetic model. The experimental data showed the best fit with the highest correlation coefficients for the pseudo-second-order model for both the PAHs. The results of the inspection are shown in Table 5. The plots of the linearized form of pseudo-second-order model (t/q_t vs. t) are given in Figs. S1–S4. From the parameters shown in Table 5, due to its higher correlation coefficient (R^2), it indicates that the adsorption kinetics follows the pseudo-second-order kinetic model much better, which also indicates that the adsorption is a fast cycle [50]. Based on the pseudo-secondary model [51], it can be well speculated that the adsorption of PAHs on wPET/C/Bt and wPS/C/Bt is chemical adsorption, and the adsorption process may involve multiple steps.

3.4. Isotherm study

To further understand the adsorption components and quantitatively describe the adsorption limit, the Freundlich and Langmuir isotherm models were used to analyze the adsorption data. The calculated Langmuir constants (k_1 and q_m) as well as the coefficients of correlation (R^2) for Langmuir isotherms are detailed in Table 6. The outcomes

uncovered that the adsorption data were better fit to the Langmuir adsorption isotherms, which were firmly identified with Langmuir model parameters in other reported investigations [52]. Figs. S5–S8 show the Langmuir isotherm plots for the adsorption of PAHs onto wPS/C/Bt and wPET/C/Bt, respectively.

3.5. Thermodynamic studies

For the adsorption of PAHs, over wPET/C/Bt and wPS/Bt, various thermodynamic parameters were studied at different temperatures. The values of $\Delta H°$, $\Delta G°$ as well as $\Delta S°$ are given in Tables 7 and 8. The positive values of $\Delta S°$ and $\Delta H°$ show the endothermic nature of PAHs onto wPS/C/Bt and wPET/C/Bt, these values show that the process is endothermic and high temperature will favor the rate of adsorption, which was also reported in the literature [53]. The adsorption process is non-spontaneous which was confirmed by the positive values of $\Delta G°$.

3.6. Vehicle wash wastewater treatment

Vehicle washing as well as maintenance are one of the most advanced petrochemical and chemical operations. This overhaul includes the evacuation of dirt, oil, particles and traffic grime by means of degreasing solvents and surfactants. Later, automobiles are presented with the utilization of petroleum and waxes products to resist the corrosion of dust and dirt [60]. The washing station is very keen to convert a large amount of clean water into wastewater containing oil-based commodities and toxic synthetic substances, which may eventually flow into the ocean and cause harm to the marine environment [61]. Wastewater from vehicle washes includes oil-based commodities such as lubricating oils, greases, engine oils, diesel, and gasoline,

Table 5
Pseudo-second-order kinetic parameters for adsorption of PAHs over wPET/C/Bt and wPS/C/Bt

PAHs	wPET/C/Bt			wPS/C/Bt		
	k_2 (mg/g min)	q_{e2} (mg/g)	R^2	k_2 (mg/g min)	q_{e2} (mg/g)	R^2
Nap	1.5291E-05	0.01	0.998	1.89E-05	0.01168	0.999
Ace	0.000159375	0.014023869	1	0.00024	0.01446	1
Acy	6.04356E-05	0.0169572	0.999	7.47E-05	0.0174	0.999
Ant	0.00012471	0.010852461	0.999	0.00023	0.01117	1
Ph	5.46598E-06	0.007556294	0.999	6.63E-06	0.00774	0.999
Fl	1.13971E-06	0.004574147	0.997	1.38E-06	0.00469	0.997
Flu	1.23564E-06	0.004636284	0.999	1.53E-06	0.00476	0.999
BaA	6.47181E-07	0.006194252	0.994	7.51E-07	0.00617	0.998
Chr	4.8967E-07	0.004701457	0.988	6.08E-07	0.00481	0.988
Pyr	1.02601E-06	0.005244939	0.999	1.23E-06	0.00536	0.999
BaP	4.53729E-07	0.004845196	0.984	5.65E-07	0.00494	0.984
BkF	2.88256E-06	0.006807352	0.998	3.52E-06	0.00697	0.998
BbF	8.27656E-07	0.005130573	0.984	1.04E-06	0.00526	0.999
D[ah]A	1.24614E-06	0.00596374	0.998	1.58E-06	0.00612	0.999
B[ghi]P	1.87446E-06	0.006896552	0.999	2.26E-06	0.00704	0.998
InP	2.00731E-06	0.008507742	0.999	2.36E-06	0.00855	1

Table 6
Isotherm model parameters for PAHs adsorption over wPET/C/Bt and wPS/C/Bt

PAHs	Langmuir isotherm parameters			Langmuir isotherm parameters		
	wPET/C/Bt			wPS/C/Bt		
	q_m (mg/g)	k_1	R^2	q_m (mg/g)	k_1	R^2
Nap	0.005	2.17×10^3	0.961	0.004	2.86×10^3	0.948
Ace	0.006	6.30×10^2	0.987	0.004	4.02×10^3	0.953
Acy	0.008	7.49×10^2	0.980	0.007	9.46×10^3	0.973
Ant	0.005	2.90×10^3	0.962	0.005	8.03×10^2	0.982
Ph	0.003	2.01×10^3	0.979	0.003	2.62×10^3	0.973
Fl	0.002	1.80×10^3	0.979	0.002	2.43×10^3	0.978
Flu	0.002	3.69×10^3	0.990	0.002	4.50×10^3	0.983
BaA	0.002	2.78×10^3	0.997	0.002	4.32×10^3	0.982
Chr	0.002	2.71×10^3	0.986	0.002	3.54×10^3	0.982
Pyr	0.003	2.24×10^3	0.983	0.003	2.37×10^3	0.992
BaP	0.003	1.91×10^3	0.988	0.003	2.43×10^3	0.984
BkF	0.003	1.86×10^3	0.992	0.003	2.28×10^3	0.987
BbF	0.004	2.8×10^3	0.984	0.002	3.85×10^3	0.983
D[ah]A	0.003	2.82×10^3	0.954	0.002	4.11×10^3	0.947
B[ghi]P	0.004	1.33×10^3	0.992	0.004	1.64×10^3	0.988
InP	0.004	1.16×10^3	0.984	0.004	1.48×10^3	0.980

which are washed away from the engine in addition to the surface of the vehicle [62].

The existence of PAHs in car wash wastewater has been investigated, which is a problem worthy of attention [63]. Wastewater from vehicle washing, such as cars, trucks, and many types of vehicles, can introduce a variety of pollutants, especially various hydrocarbons, chemicals, greases, oils, phosphates, and detergents. Contaminants in this wastewater can not only affect the quality of surface water, they can also be dangerous to aquatic life, although groundwater may be marked as undrinkable due to elevated concentrations [62]. Oily wastewater contains harmful organic compounds, such as PAHs, phenol, and petroleum hydrocarbons, which can hinder the growth of animals and plants, and cause carcinogenesis and mutagenic effects on humans [64].

In this study, the composite adsorbents such as wPET/C/Bt as well as wPS/C/Bt were also utilized for PAHs adsorption from vehicle wash wastewater through batch adsorption experiment. For this purposes the vehicle wash wastewater samples from both heavy vehicle-wash stations (buses, trailers, trucks, and oil carriages) as well as light vehicle-wash stations (pickups, mini coaches, cars etc.) were collected and homogenized in pre-cleaned 2.5 L amber glass bottles. The experimental results show that for wPET/C/Bt under the optimal conditions (0.8 g adsorbent dose, temperature 50°C, 1 h contact time, 6 pH, and 40 ppm concentration), the highest % adsorption rate of Nap, Ace, Acy, Ant, Ph, Fl, Flu, BaA, Chr, Pyr, BaP, BkF, BbF, D[ah]A, B[ghi]P, InP was 78.44, 76.36, 82.74, 86.54, 81.04, 86.52, 77.73, 81.85, 78.47, 77.80, 80.83, 79.16, 83.08, 85.82, 79.83, 84.49, respectively (Fig. 7). Similarly, for wPS/C/Bt under the optimal conditions (0.8 g adsorbent dose, temperature 50°C, 1 h contact time, 6 pH, and 40 ppm concentration), the highest % adsorption rate of Nap, Ace, Acy, Ant,

Ph, Fl, Flu, BaA, Chr, Pyr, BaP, BkF, BbF, D[ah]A, B[ghi]P, InP was 76.03, 71.82, 77.92, 78.06, 73.75, 77.08, 81.44, 82.12, 76.72, 76.52, 77.49, 78.65, 74.57, 77.51, 78.96, 81.67, respectively (Fig. 6). The findings of this study show that wPET/C/Bt and wPS/C/Bt may be promising adsorbents that can effectively remove PAHs from vehicle wash wastewater.

3.7. Comparison of adsorption potential of different adsorbents

Table 9 summarizes the comparative adsorption efficiencies of adsorbents, that is, wPET/C/Bt and wPS/C/Bt and various adsorption media reported in the literature used for PAHs adsorption.

3.8. Mechanisms of PAHs adsorption

Lyklema [65] reported that the PAHs adsorption from aqueous solution is basically an exchange process. Therefore, the adsorption process of organic compounds on the surface of composite adsorbent has been described as a complex interaction between electrostatic and dispersion interactions, especially in the case of weak organic electrolytes. However, since PAHs are not considered to be electrolytic, the intermediate hydrogen bonding as well as van der Waals dispersive interactions have become the main mechanisms proposed in the literature [66].

3.9. Desorption and reusability

In the adsorption processes, desorption/regeneration of adsorbents is one of the essential aspects as it controls the economy of water treatment technology [67]. In this study, HCl solution was used for the desorption experiment. Acid gave satisfactory desorption results. The regeneration

Table 7
Thermodynamic factors for the adsorption of PAHs onto wPS/C/Bt

Temperature (°C)	$\Delta G°$ (kJ/mol)	$\Delta H°$ (kJ/mol)	$\Delta S°$ (kJ/mol)	$\Delta G°$ (kJ/mol)	$\Delta H°$ (kJ/mol)	$\Delta S°$ (kJ/mol)
	Nap			Ace		
			wPS/C/Bt			
20	8.98			9.59		
30	7.83	44.07	0.12	7.99	50.32	0.14
40	7.36			6.54		
50	5.12			5.45		
	Acy			Ant		
20	8.44			7.90		
30	8.19	47.82	0.13	7.05	53.22	0.15
40	7.00			4.86		
50	4.33			3.48		
	Ph			Fl		
20	8.29			8.03		
30	7.01	42.97	0.12	6.31	52.44	0.15
40	6.04			4.82		
50	4.66			3.48		
	Flu			BaA		
20	8.17			8.64		
30	6.79	36.47	0.10	6.23	49.07	0.14
40	5.97			4.93		
50	5.24			4.51		
	Chr			Pyr		
20	8.16			7.66		
30	7.08	38.69	0.10	6.13	32.47	0.08
40	5.82			5.07		
50	5.11			5.22		
	BaP			BkF		
20	8.14			7.91		
30	7.25	44.62	0.12	7.14	38.39	0.11
40	5.20			5.52		
50	4.70			5.00		
	BbF			D[ah]A		
20	8.89			9.59		
30	6.01	52.14	0.15	7.47	71.13	0.21
40	5.19			4.40		
50	4.26			3.66		
	B[ghi]P			InP		
20	7.700			8.09		
30	6.60	37.11	0.10	6.81	50.64	0.14
40	5.10			4.72		
50	4.88			3.96		

Table 8
Thermodynamic factors for the adsorption of PAHs onto wPS/C/Bt

Temperature (°C)	$\Delta G°$ (kJ/mol)	$\Delta H°$ (kJ/mol)	$\Delta S°$ (kJ/mol)	$\Delta G°$ (kJ/mol)	$\Delta H°$ (kJ/mol)	$\Delta S°$ (kJ/mol)
		Nap			Ace	
		wPS/C/Bt				
20	8.577			9.15		
30	7.51	45.94	0.13	7.67	48.49	0.13
40	7.02			6.17		
50	4.44			5.19		
		Acy			Ant	
20	8.03			7.49		
30	7.88	50.17	0.14	6.71	53.84	0.16
40	6.66			4.33		
50	3.59			3.02		
		Ph			Fl	
20	7.88			7.62		
30	6.67	44.21	0.12	5.94	42.65	0.12
40	5.64			4.28		
50	4.09			4.23		
		Flu			BaA	
20	7.76			8.23		
30	6.44	38.71	0.13	7.00	46.48	0.13
40	5.56			5.95		
50	3.70			4.22		
		Chr			Pyr	
20	7.75			7.24		
30	6.74	38.71	0.10	5.75	35.20	0.10
40	5.40			4.91		
50	4.69			4.36		
		BaP			BkF	
20	7.74			7.50		
30	6.92	45.99	0.13	6.80	44.36	0.12
40	4.72			5.07		
50	4.14			3.89		
		BbF			D[ah]A	
20	8.47			9.15		
30	5.61	43.02	0.12	7.15	58.07	0.17
40	5.19			5.54		
50	4.72			4.14		
		B[ghi]P			InP	
20	7.29			7.68		
30	6.24	42.74	0.12	6.46	54.53	0.16
40	4.60			4.17		
50	3.82			3.13		

wPET/C/Bt **wPS/C/Bt**

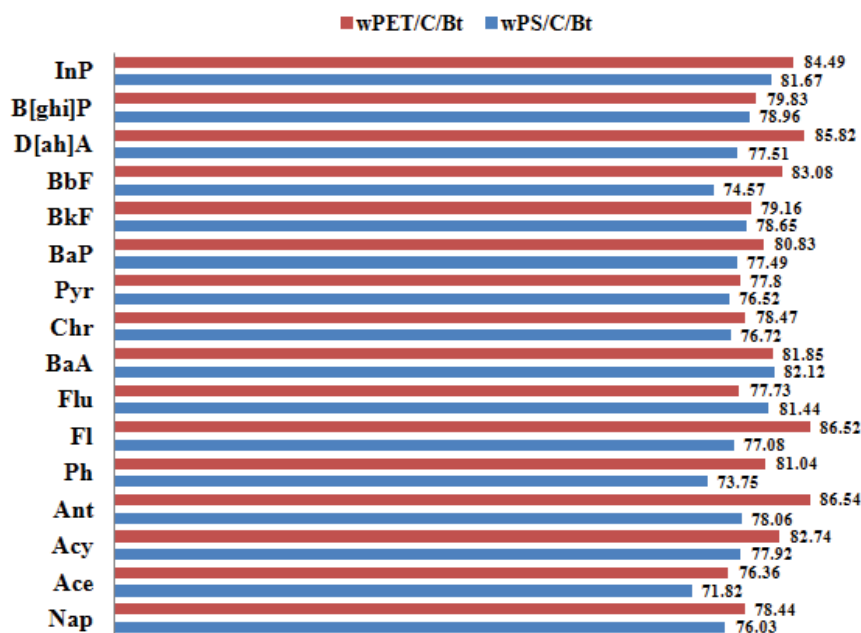| PAH	wPS/C/Bt	wPET/C/Bt
InP	81.67	84.49
B[ghi]P	78.96	79.83
D[ah]A	77.51	85.82
BbF	74.57	83.08
BkF	78.65	79.16
BaP	77.49	80.83
Pyr	76.52	77.8
Chr	76.72	78.47
BaA	82.12	81.85
Flu	81.44	77.73
Fl	77.08	86.52
Ph	73.75	81.04
Ant	78.06	86.54
Acy	77.92	82.74
Ace	71.82	76.36
Nap	76.03	78.44

Fig. 7. Adsorptions of PAHs from vehicle wash wastewater using composite adsorbents under different experiment conditions.

wPET/C/Bt **wPS/C/Bt**

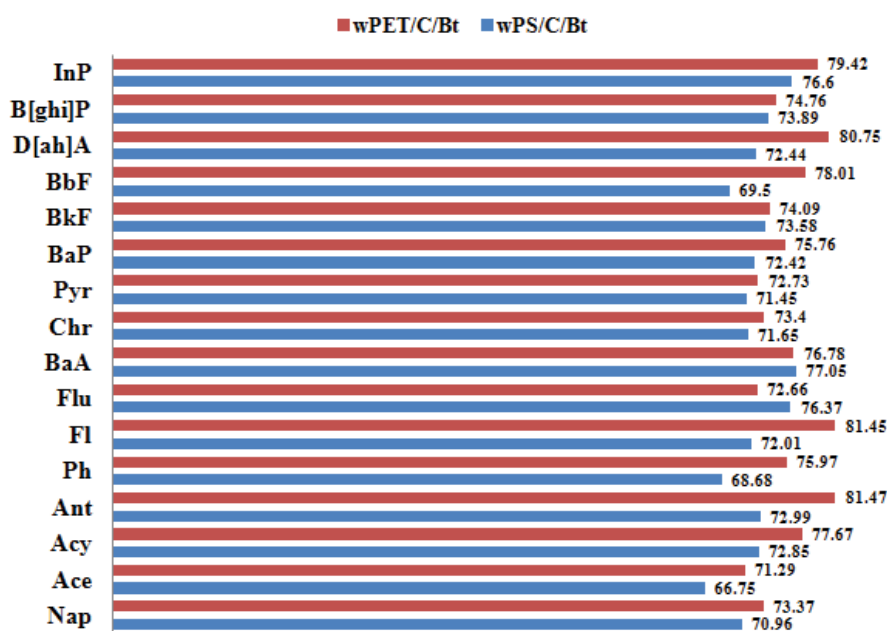| PAH	wPS/C/Bt	wPET/C/Bt
InP	76.6	79.42
B[ghi]P	73.89	74.76
D[ah]A	72.44	80.75
BbF	69.5	78.01
BkF	73.58	74.09
BaP	72.42	75.76
Pyr	71.45	72.73
Chr	71.65	73.4
BaA	77.05	76.78
Flu	76.37	72.66
Fl	72.01	81.45
Ph	68.68	75.97
Ant	72.99	81.47
Acy	72.85	77.67
Ace	66.75	71.29
Nap	70.96	73.37

Fig. 8. Regenerating efficiency of wPET/C/Bt and wPS/C/Bt.

studies were carried out in batch using 100 mL of standard solutions indicating that wPS/C/Bt and wPET/C/Bt had the potential for reusability (Fig. 8).

4. Conclusion

In the current study, waste plastics such as wPS and wPET have been successfully used to prepare composite adsorbents through simple as well as economical methods.

Synthetic composite adsorbents wPS/C/Bt and wPET/C/Bt were used for PAHs adsorption from wastewater as well as aqueous solution by batch adsorption method. The process of PAHs adsorption completely depends on temperature, initial PAHs concentrations, contact time, pH value as well as the amount of adsorbents. The adsorption process proceeds and conforms to the Langmuir isotherm as well as pseudo-second-order equation. Thermodynamic studies show that the adsorption process is an endothermic

Table 9
Details of adsorption media and their PAHs removal efficiency

Materials	Study type	PAHs % removal effectiveness	Sorption isotherm model	References
wPS/C/Bt	Batch	Nap (77.43), Ace (73.22), Acy (79.32), Ant (79.46), Ph (75.15), Fl (78.48), Flu (82.84), BaA (83.52), Chr (78.12), Pyr (77.92), BaP (78.89), BkF (80.05), BbF (75.97), D[ah]A (78.91), B[ghi]P (80.36), InP (83.07)	Langmuir	This article
wPET/C/Bt	Batch	Nap (81.98), Ace (79.72), Acy (86.56), Ant (88.04), Ph (84.30), Fl (87.55), Flu (80.84), BaA (84.92), Chr (82.20), Pyr (81.28), BaP (83.89), BkF (82.52), BbF (85.97), D[ah]A (88.22), B[ghi]P (81.34), InP (88.26)	Langmuir	This article
wPS-AC	Batch	Nap (90.61), Ace (89.40), Acy (92.50), Ant (94.64), Ph (95.33), Fl (94.66), Flu (96.02), BaA (94.7), Chr (92.3), Pyr (94.10), BaP (95.07), BkF (96.23), BbF (92.15), D[ah]A (90.01), B[ghi]P (96.54), InP (93.25)	Langmuir and Freundlich,	[35]
wPET-AC	Batch	Nap (96.22), Ace (94.67), Acy (97.21), Ant (98.22), Ph (93.65), Fl (97.31), Flu (94.02), BaA (92.10), Chr (90.31), Pyr (93.46), BaP (92.23), BkF (93.25), BbF (94.49), D[ah]A (95.09), B[ghi]P (91.54), InP (96.47)	Langmuir and Freundlich,	[35]
Powder activated carbon anthracite-based and coconut shells based	Batch	BbF (86), Ph (95), Chr (94.5), BaP (88), Flu (96.5), Pyr (98), BaA (94.5), InP (73), BkF (88), B[ghi]P (69), Ant (97.5)	Freundlich	[54]
Wood char	Batch	Pyr, Ph, BaA (≥60)	Freundlich	[55]
Aspen wood fiber	Batch/Column	Pyr (74), Ant (67), Fl (25.5)	Freundlich	[56]
Inorgano–organo-bentonite	Batch	Ph (99)	Langmuir	[57]
Activated carbon	Batch	>97% Nap and >98% Flu	Langmuir and Freundlich	[42]
Wood ashes	Batch	B[ghi]P, Fl, Pyr, BaP, Chr, BaA, BbF, D[ah]A, BkF, InP (>99)	Freundlich	[58]
Coke-derived porous carbon	Batch	Nap, Fl, Ph, Pyr, Flu (>99 for all PAHs)	Freundlich	[59]

non-spontaneous process. This finding indicates that wPS/C/Bt in addition to wPET/C/Bt is very efficient adsorbents for the adsorption of PAHs from wastewater.

References

[1] E. Mine Öncü Kaya, A. Safa Özcan, Ö. Gök, A. Özcan, Adsorption kinetics and isotherm parameters of naphthalene onto natural- and chemically modified bentonite from aqueous solutions, Adsorption, 19 (2013) 879–888.

[2] H.I. Abdel-Shafy, MS.M. Mansour, A review on polycyclic aromatic hydrocarbons: source, environmental impact, effect on human health and remediation, Egypt. J. Pet., 25 (2016) 107–123.

[3] B. Kumar, V.K. Verma, C.S. Sharma, A.B. Akolkar, Estimation of toxicity equivalency and probabilistic health risk on lifetime daily intake of polycyclic aromatic hydrocarbons from urban residential soils, Hum. Ecol. Risk Assess., 21 (2015) 434–444.

[4] R. Duran, C. Cravo-Laureau, Role of environmental factors and microorganisms in determining the fate of polycyclic aromatic hydrocarbons in the marine environment, FEMS Microbiol. Rev., 40 (2016) 814–830.

[5] A. Forsgren, Wastewater Treatment: Occurrence and Fate of Polycyclic Aromatic Hydrocarbons (PAHs), Taylor & Francis, Boca Raton, New York, London, 2015.

[6] R.G. Harvey, Polycyclic Aromatic Hydrocarbons, Wiley-VCH, New York, 1997.

[7] M. Hedayati, Removal of Polycyclic Aromatic Hydrocarbons From Deionized Water and Landfill Leachate by Using Modified Clinoptilolites, Doctoral Dissertation, University of British Columbia.

[8] C. Lin, L. Gan, Z.-L. Chen, Biodegradation of naphthalene by strain *Bacillus fusiformis* (BFN), J. Hazard. Mater., 182 (2010) 771–777.

[9] E. Mine Öncü Kaya, A. Safa Özcan, Ö. Gök, A. Özcan, Adsorption kinetics and isotherm parameters of naphthalene onto natural- and chemically modified bentonite from aqueous solutions, Adsorption, 19 (2013) 879–888.

[10] Y.-H. Chuang, C.-H. Liu, Y.-M. Tzou, J.-S. Chang, P.-N. Chiang, M.-K. Wang, Comparison and characterization of chemical surfactants and bio-surfactants intercalated with layered double hydroxides (LDHs) for removing naphthalene from contaminated aqueous solutions, Colloids Surf., A, 366 (2010) 170–177.

[11] W. Zhou, X. Wang, C. Chen, L. Zhu, Removal of polycyclic aromatic hydrocarbons from surfactant solutions by selective sorption with organo-bentonite, Chem. Eng. J., 233 (2013) 251–257.

[12] Y. Hu, Y. He, X. Wang, C. Wei, Efficient adsorption of phenanthrene by simply synthesized hydrophobic MCM-41 molecular sieves, Appl. Surf. Sci., 311 (2014) 825–830.

[13] C.-H. Li, Y.-S. Wong, H.-Y. Wang, N.F.-Y. Tam, Anaerobic biodegradation of PAHs in mangrove sediment with amendment of NaHCO₃, J. Environ. Sci., 30 (2015) 148–156.

[14] H. Li, R. Qu, C. Li, W. Guo, X. Han, F. He, Y. Ma, B. Xing, Selective removal of polycyclic aromatic hydrocarbons (PAHs) from soil washing effluents using biochars produced at different pyrolytic temperatures, Bioresour. Technol., 163 (2014) 193–198.

[15] R.-H. Peng, X.-Y. Fu, W. Zhao, Y.-S. Tian, B. Zhu, H.-J. Han, J. Xu, Q.-H. Yao, Phytoremediation of phenanthrene by transgenic plants transformed with a naphthalene dioxygenase system from *Pseudomonas*, Environ. Sci. Technol., 48 (2014) 12824–12832.

[16] K. Sun, J. Liu, Y. Gao, L. Jin, Y. Gu, W. Wang, Isolation, plant colonization potential and phenanthrene degradation performance of the endophytic bacterium *Pseudomonas* sp. Ph6-*gfp*, Sci. Rep., 4 (2014) 5462, doi: 10.1038/srep05462.

[17] I. Ali, Mohd. Asim, T.A. Khan, Low cost adsorbents for the removal of organic pollutants from wastewater, J. Environ. Manage., 113 (2012) 170–183.

[18] J. Mittal, A. Mittal, H. Feather, A Remarkable Adsorbent for Dye Removal. Green Chemistry for Dyes Removal from Wastewater, Scrivener Publishing LLC, USA, 2015, pp. 409–457.

[19] D. Pan, S. Ge, J. Zhao, J. Tian, Q. Shao, L. Guo, X. Mai, T. Wu, V. Murugadoss, H. Liu, T. Ding, S. Angaiah, Z. Guo, Synthesis and characterization of ZnNiIn layered double hydroxides derived mixed metal oxides with highly efficient photoelectrocatalytic activities, Ind. Eng. Chem. Res., 58 (2018) 836–848.

[20] S. Soni, P.K. Bajpai, J. Mittal, C. Arora, Utilisation of cobalt doped Iron based MOF for enhanced removal and recovery of methylene blue dye from waste water, J. Mol. Liq., 314 (2020) 113642, doi: 10.1016/j.molliq.2020.113642.

[21] I. Anastopoulos, I. Pashalidis, A.G. Orfanos, I.D. Manariotis, T. Tatarchuk, L. Sellaoui, A. Bonilla-Petriciolet, A. Mittal, A. Núñez-Delgado, Removal of caffeine, nicotine and amoxicillin from (waste)waters by various adsorbents. A review, J. Environ. Manage., 261 (2020) 110236, doi: 10.1016/j.jenvman.2020.110236.

[22] R. Jain, P. Sharma, S. Sikarwar, J. Mittal, D. Pathak, Adsorption kinetics and thermodynamics of hazardous dye Tropaeoline 000 unto Aeroxide Alu C (Nano alumina): a non-carbon adsorbent, Desal. Water Treat., 52 (2014) 7776–7783.

[23] S. Soni, P.K. Bajpai, D. Bharti, J. Mittal, C. Arora, Removal of crystal violet from aqueous solution using iron based metal organic framework, Desal. Water Treat., 205 (2020) 386–399.

[24] H. Daraei, A. Mittal, Investigation of adsorption performance of activated carbon prepared from waste tire for the removal of methylene blue dye from wastewater, Desal. Water Treat., 90 (2017) 294–298.

[25] R. Ahmad, I. Hasan, A. Mittal, Adsorption of Cr(VI) and Cd(II) on chitosan grafted polyaniline-OMMT nanocomposite: isotherms, kinetics and thermodynamics studies, Desal. Water Treat., 58 (2017) 144–153.

[26] J. Mittal, R. Ahmad, A. Mariyam, V.K. Gupta, A. Mittal, Expeditious and enhanced sequestration of heavy metal ions from aqueous environment by papaya peel carbon: a green and low-cost adsorbent, Desal. Water Treat., 210 (2021) 365–376.

[27] A. Mittal, R. Ahmad, I. Hasan, Iron oxide-impregnated dextrin nanocomposite: synthesis and its application for the biosorption of Cr(VI) ions from aqueous solution, Desal. Water Treat., 57 (2016) 15133–15145.

[28] C. Vanlalveni, S. Lallianrawna, A. Biswas, M. Selvaraj, B. Changmai, S.L. Rokhum, Green synthesis of silver nanoparticles using plant extracts and their antimicrobial activities: a review of recent literature, RSC Adv., 11 (2016) 2804–2837.

[29] N.M. Alandis, W. Mekhamer, O. Aldayel, J.A.A. Hefne, M. Alam, Adsorptive applications of montmorillonite clay for the removal of Ag(I) and Cu(II) from aqueous medium, J. Chem., 2019 (2019) 7129014, doi: 10.1155/2019/7129014.

[30] A. Mittal, R. Ahmad, I. Hasan, Poly(methyl methacrylate)-grafted alginate/Fe₃O₄ nanocomposite: synthesis and its application for the removal of heavy metal ions, Desal. Water Treat., 57 (2016) 19820–19833.

[31] A. Mittal, R. Ahmad, I. Hasan, Biosorption of Pb²⁺, Ni²⁺ and Cu²⁺ ions from aqueous solutions by L-cystein-modified montmorillonite-immobilized alginate nanocomposite, Desal. Water Treat., 57 (2016) 17790–17807.

[32] M. Ilyas, W. Ahmad, H. Khan, S. Yousaf, Potentially poisonous elements removal from vehicle wash wastewater and aqueous solutions using composite adsorbents, Desal. Water Treat., 224 (2021) 331–342.

[33] M. Ilyas, W. Ahmad, H. Khan, I. Ahmad, Application of composite adsorbents prepared from waste PS and PET for removal of Cr and Cu ions from wastewater, Desal. Water Treat., 171 (2019) 144–157.

[34] M. Ilyas, W. Ahmad, H. Khan, Utilization of activated carbon derived from waste plastic for decontamination of polycyclic aromatic hydrocarbons laden wastewater, Water Sci. Technol., 84 (2021) 609–631.

[35] M. Ilyas, W. Ahmad, H. Khan, Polycyclic aromatic hydrocarbons removal from vehicle wash wastewater using activated char, Desal. Water Treat., 236 (2021b) 55–68.

[36] E. Mansouri, V. Yousefi, V. Ebrahimi, S. Eyvazi, M.S. Hejazi, M. Mahdavi, M. Asghar, V. Tarhriz, Overview of ultraviolet-based methods used in polycyclic aromatic hydrocarbons analysis and measurement, Sep. Sci., 3 (2020) 112–120.

[37] R.M. Silverstein, F.X. Webster, 13C NMR Spectrometry, in: Spectrometric Identification of Organic Compounds, 1998, pp. 217–249.

[38] M. Chollet, M. Horgnies, Analyses of the surfaces of concrete by Raman and FT-IR spectroscopies: comparative study of hardened samples after demoulding and after organic post-treatment, Surf. Interface Anal., 43 (2011) 714–725.

[52] V. Hermán, V. Takacs, F. Duclairoir, O. Renault, J.H. Tortai, B. Viala, Core double–shell cobalt/graphene/polystyrene magnetic nanocomposites synthesized by *in situ* sonochemical polymerization, RSC Adv., 5 (2015) 51371–51381.

[40] M. Subramani, U. Sepperumal, FTIR analysis of bacterial mediated chemical changes in polystyrene foam, Ann. Biol. Res., 7 (2016) 55–61.

[41] H. Liu, S. Liang, J.H. Gao, H.H. Ngo, W.S. Guo, Z.Z. Guo, J. Wang, Y.R. Li, Enhancement of Cr(VI) removal by modifying activated carbon developed from *Zizania caduciflora* with tartaric acid during phosphoric acid activation, Chem. Eng. J., 246 (2014) 168–174.

[42] A. Awoyemi, Understanding the Adsorption of Polycyclic Aromatic Hydrocarbons from Aqueous Phase onto Activated Carbon (Doctoral Dissertation), 2011.

[43] R. Moradi-Rad, L. Omidi, L.H. Kakooei, F. Golbabaei, H. Hassani, R. Abedin-Loo, K. Azam, Adsorption of polycyclic aromatic hydrocarbons on activated carbons: kinetic and isotherm curve modeling, Int. J. Occup. Hyg., 6 (2014) 43–49.

[44] V.O. Njoku, M.A. Islam, M. Asif, B.H. Hameed, Utilization of sky fruit husk agricultural waste to produce high quality activated carbon for the herbicide bentazon adsorption, Chem. Eng. J., 251 (2014) 183–191.

[45] S. Chen, J. Zhang, C. Zhang, Q. Yue, Y. Li, C. Li, Equilibrium and kinetic studies of methyl orange and methyl violet adsorption on activated carbon derived from *Phragmites australis*, Desalination, 252 (2010) 149–156.

[46] A. Mittal, L. Kurup, J. Mittal, Freundlich and Langmuir adsorption isotherms and kinetics for the removal of Tartrazine from aqueous solutions using hen feathers, J. Hazard. Mater., 146 (2007) 243–248.

[47] T. Qiu, Y. Zeng, C. Ye, H. Tian, Adsorption thermodynamics and kinetics of *p*-xylene on activated carbon, J. Chem. Eng. Data, 57 (2012) 1551–1556.

[48] E.K. Putra, R, Pranowo, J. Sunarso, N. Indraswati, S. Ismadji, Performance of activated carbon and bentonite for adsorption of amoxicillin from wastewater: mechanisms, isotherms and kinetics, Water Res., 43 (2009) 2419–2430.

[49] A.F. Tajar, T. Kaghazchi, M. Soleimani, Adsorption of cadmium from aqueous solutions on sulfurized activated carbon prepared from nut shells, J. Hazard. Mater., 165 (2009) 1159–1164.

[50] Y. Hao, Z. Wang, J. Gou, S. Dong, Highly efficient adsorption and removal of Chrysoidine Y from aqueous solution by magnetic graphene oxide nanocomposite, Arabian J. Chem., 12 (2019) 3064–3074.

[51] V. Vadivelan, K.V. Kuma, Equilibrium, kinetics, mechanism, and process design for the sorption of methylene blue onto rice husk, J. Colloid Interface Sci., 286 (2005) 90–100.

[52] R.M. Shrestha, I. Varga, J. Bajtai, M. Varga, Design of surface functionalization of waste material originated charcoals by an optimized chemical carbonization for the purpose of heavy metal removal from industrial waste waters, Microchem. J., 108 (2013) 224–232.

[53] T.U. Rehman, S. Bibi, M. Khan, I. Ali, L.A. Shah, A. Khan, M. Ateeq, Fabrication of stable superabsorbent hydrogels for successful removal of crystal violet from waste water, RSC Adv., 9 (2019) 40051–40061.

[54] K. Amstaetter, E. Eek, G. Cornelissen, Sorption of PAHs and PCBs to activated carbon: coal versus biomass-based quality, Chemosphere, 87 (2012) 573–578.

[55] W. Xilong, T. Sato, B. Xing, Competitive sorption of pyrene on wood chars, Environ. Sci. Technol., 40 (2006) 3267–3272.

[56] T.B. Boving, W. Zhang, Removal of aqueous-phase polynuclear aromatic hydrocarbons using aspen wood fibers, Chemosphere, 54 (2004) 831–839.

[57] M. Jianfeng, L. Zhu, Simultaneous sorption of phosphate and phenanthrene to inorgano–organo-bentonite from water, J. Hazard. Mater., 136 (2006) 982–988.

[58] M.R. Pérez-Gregorio, M.S. García-Falcón, E. Martínez-Carballo, J. Simal-Gándara, Removal of polycyclic aromatic hydrocarbons from organic solvents by ashes wastes, J. Hazard. Mater., 178 (2010) 273–281.

[59] M. Yuan, S. Tong, S. Zhao, C.Q. Jia, Adsorption of polycyclic aromatic hydrocarbons from water using petroleum coke-derived porous carbon, J. Hazard. Mater., 181 (2010) 1115–1120.

[60] I.A. Rodriguez Boluarte, M. Andersen, B.K. Pramanik, C.-Y. Chang, S. Bagshaw, L. Farago, V. Jegatheesan, L. Shu, Reuse of car wash wastewater by chemical coagulation and membrane bioreactor treatment processes, Int. Biodeterior. Biodegrad., 113 (2016) 44–48.

[61] A. Al-Odwani, M. Ahmed, S. Bou-Hamad, Carwash water reclamation in Kuwait, Desalination, 206 (2007) 17–28.

[62] C. Sablayrolles, C. Vialle, C. Vignoles, M. Montréjaud-Vignoles, Impact of carwash discharge on stormwater quality (Toulouse, France), Water Sci. Technol., 62 (2010) 2737–2746.

[63] R. Ermens, Literature Review: Urban River Contaminants, Environment Canterbury Report U, 2007.

[64] M. Gryta, K. Karakulski, A.W. Morawski, Purification of oily wastewater by hybrid UF/MD, Water Res., 35 (2001) 3665–3669.

[65] J. Lyklema, Fundamentals of Interface and Colloid Science. Solid–liquid Interfaces, Vol. II, Academic Press, New York, 1995, p. 770.

[66] H. Gupta, Removal of phenanthrene from water using activated carbon developed from orange rind, Int. J. Sci. Res. Environ. Sci., 3 (2015) 248–255.

[67] I. Ali, New generation adsorbents for water treatment, Chem. Rev., 112 (2012) 5073–5091.
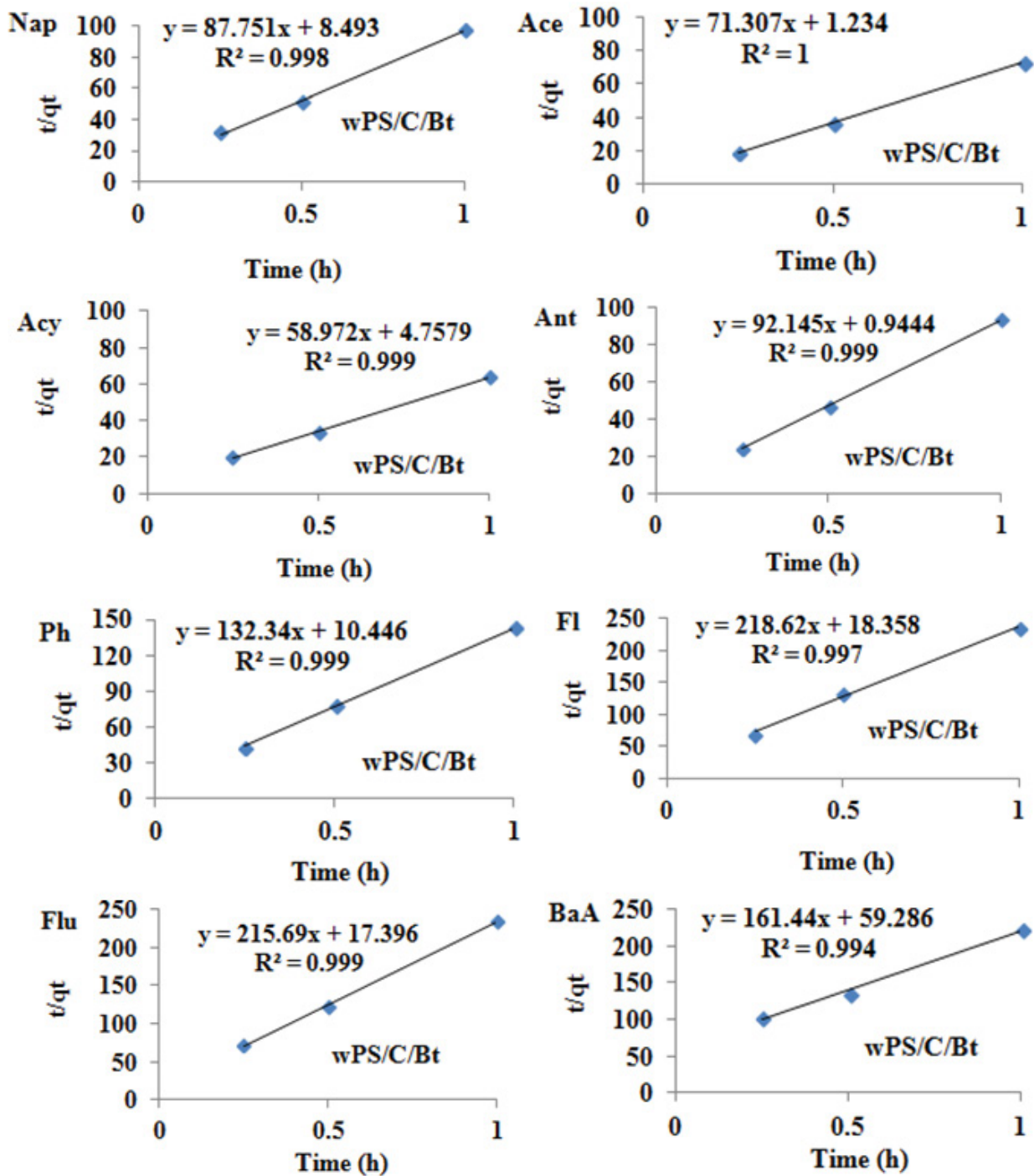
Supplementary information

Fig. S1. Plots of the pseudo-second-order kinetics for wPS/C/Bt in batch experiment.
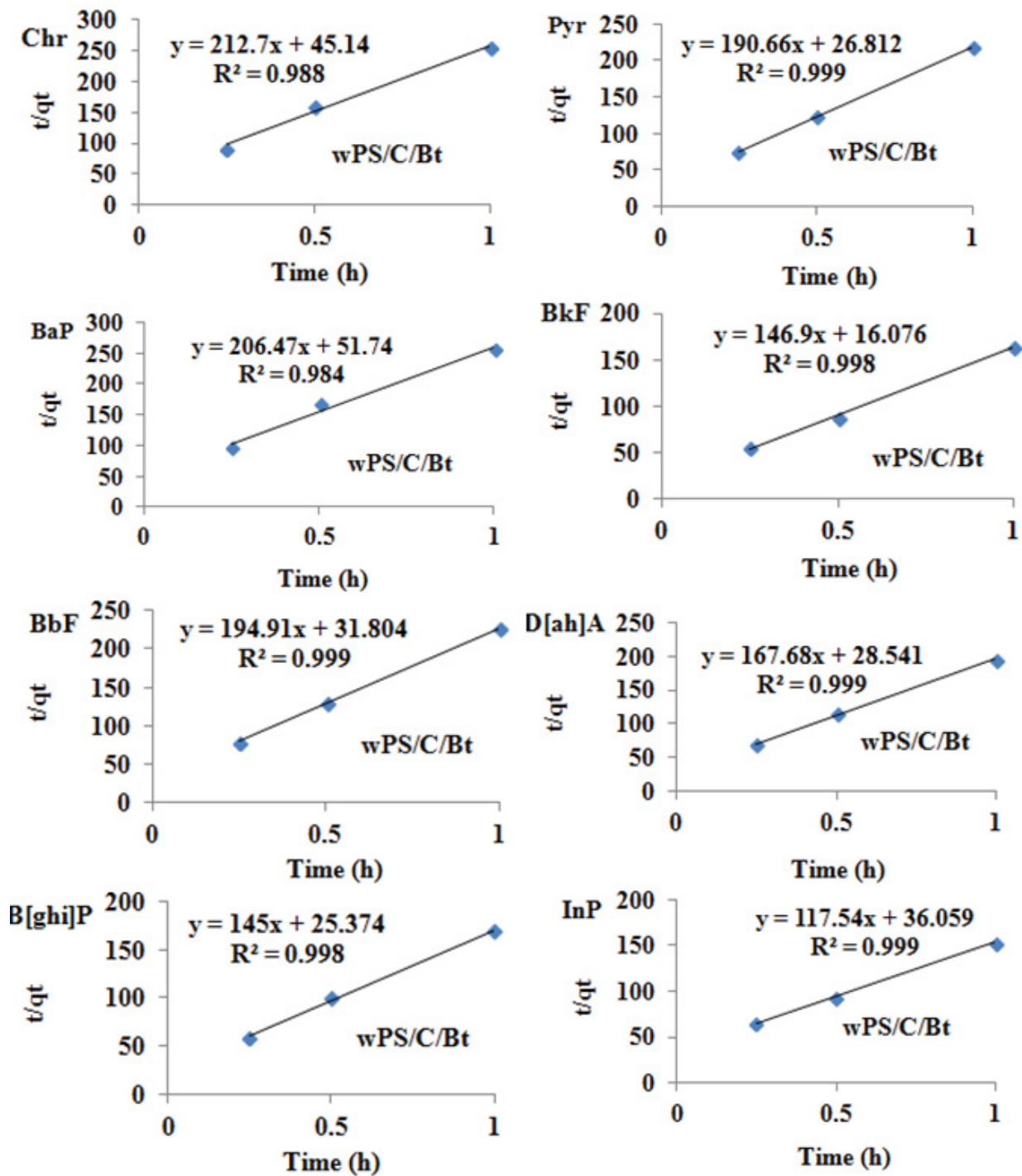
Fig. S2. Plots of the pseudo-second-order kinetics for wPS/C/Bt in batch experiment.
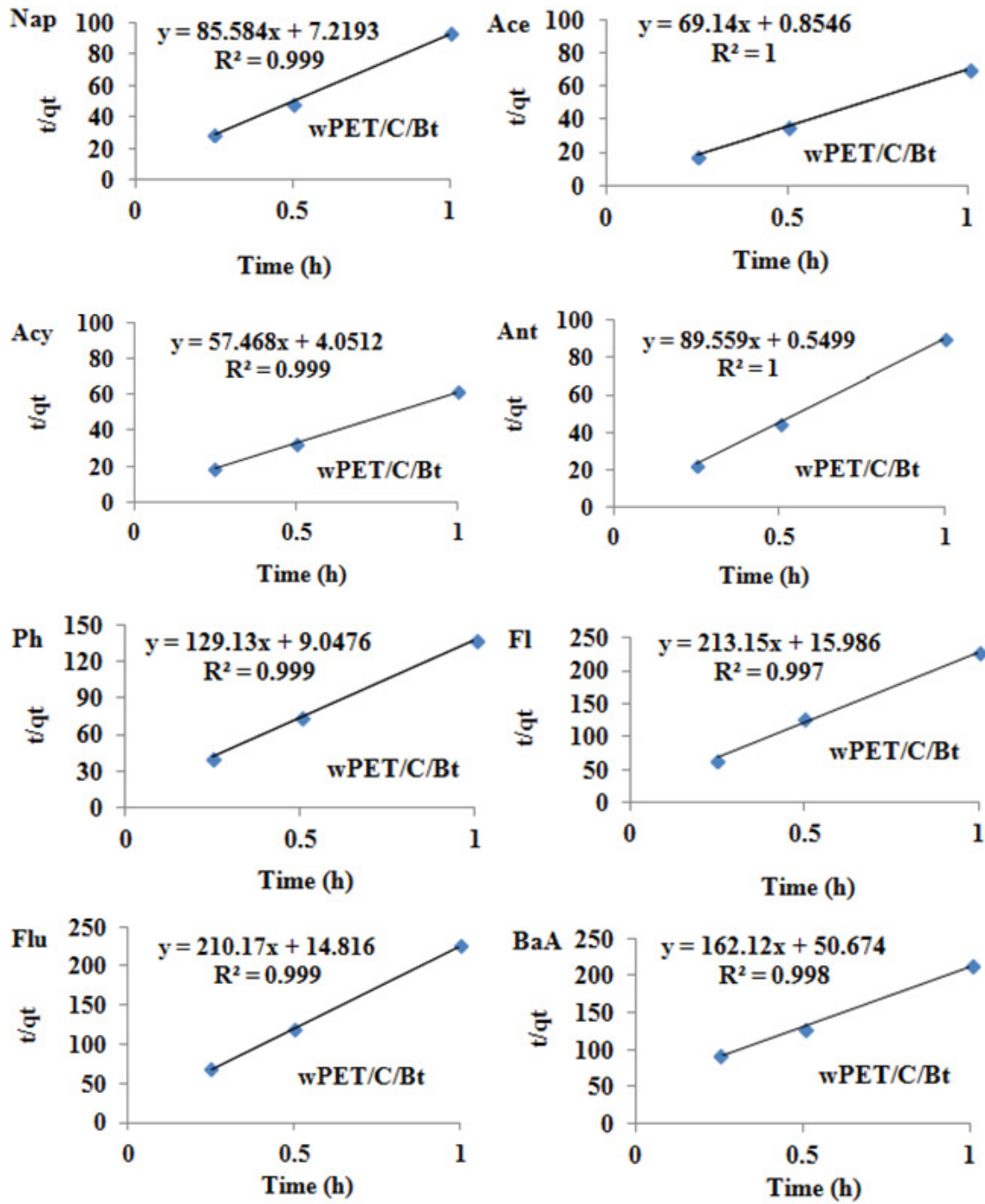
Fig. S3. Plots of the pseudo-second-order kinetics for wPET/C/Bt in batch experiment.
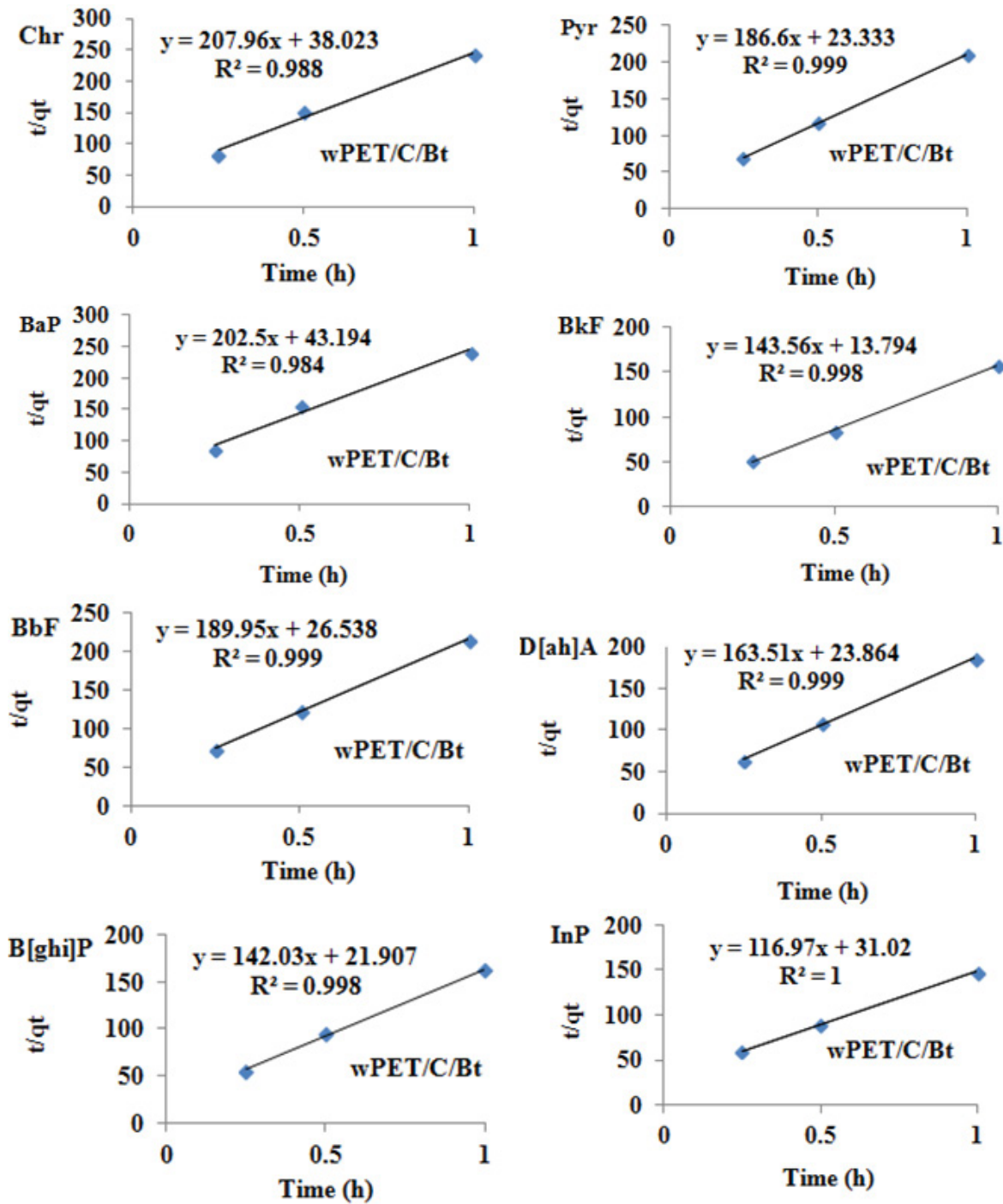
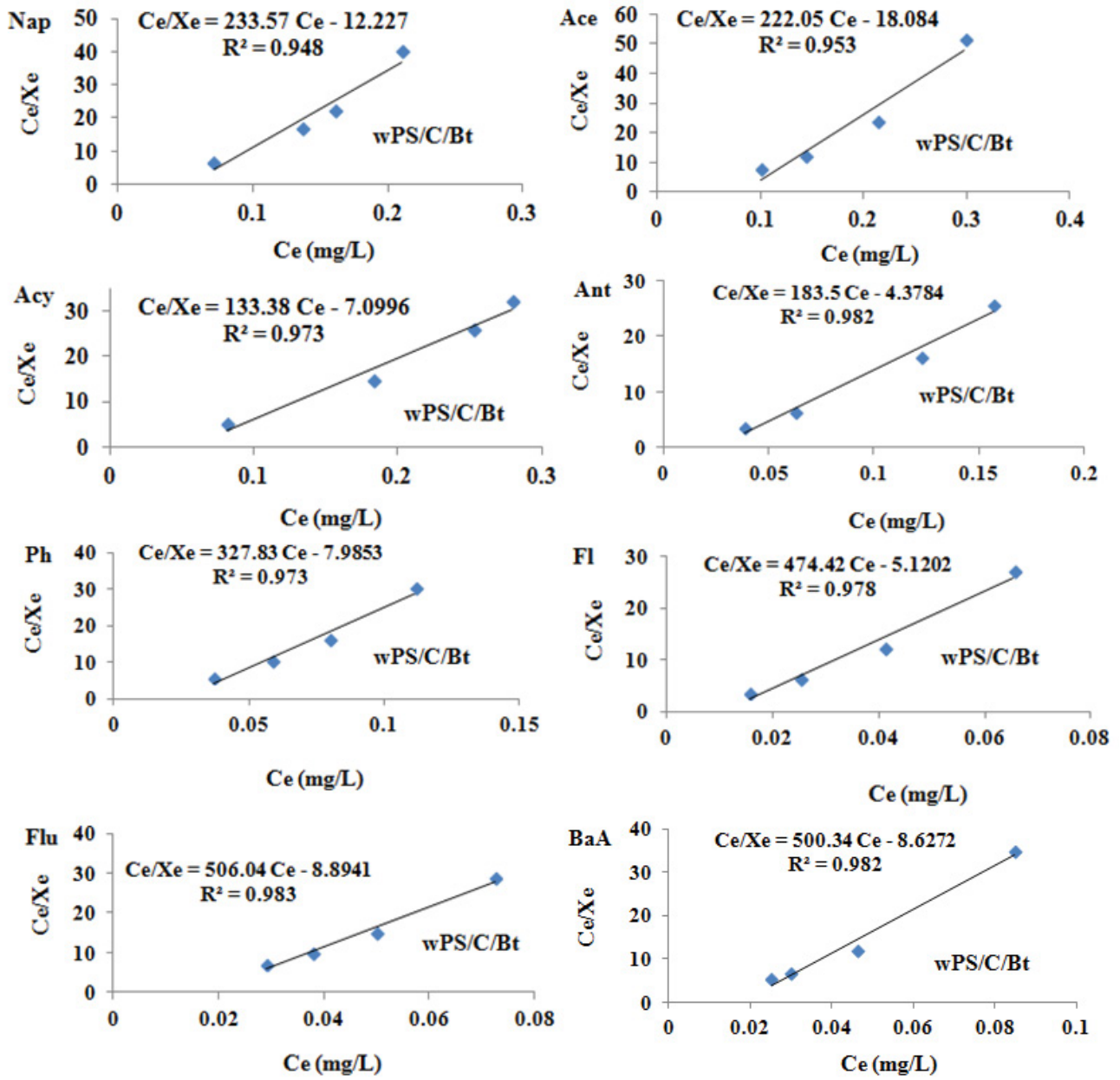Fig. S4. Plots of the pseudo-second-order kinetics for wPET/C/Bt in batch experiment.

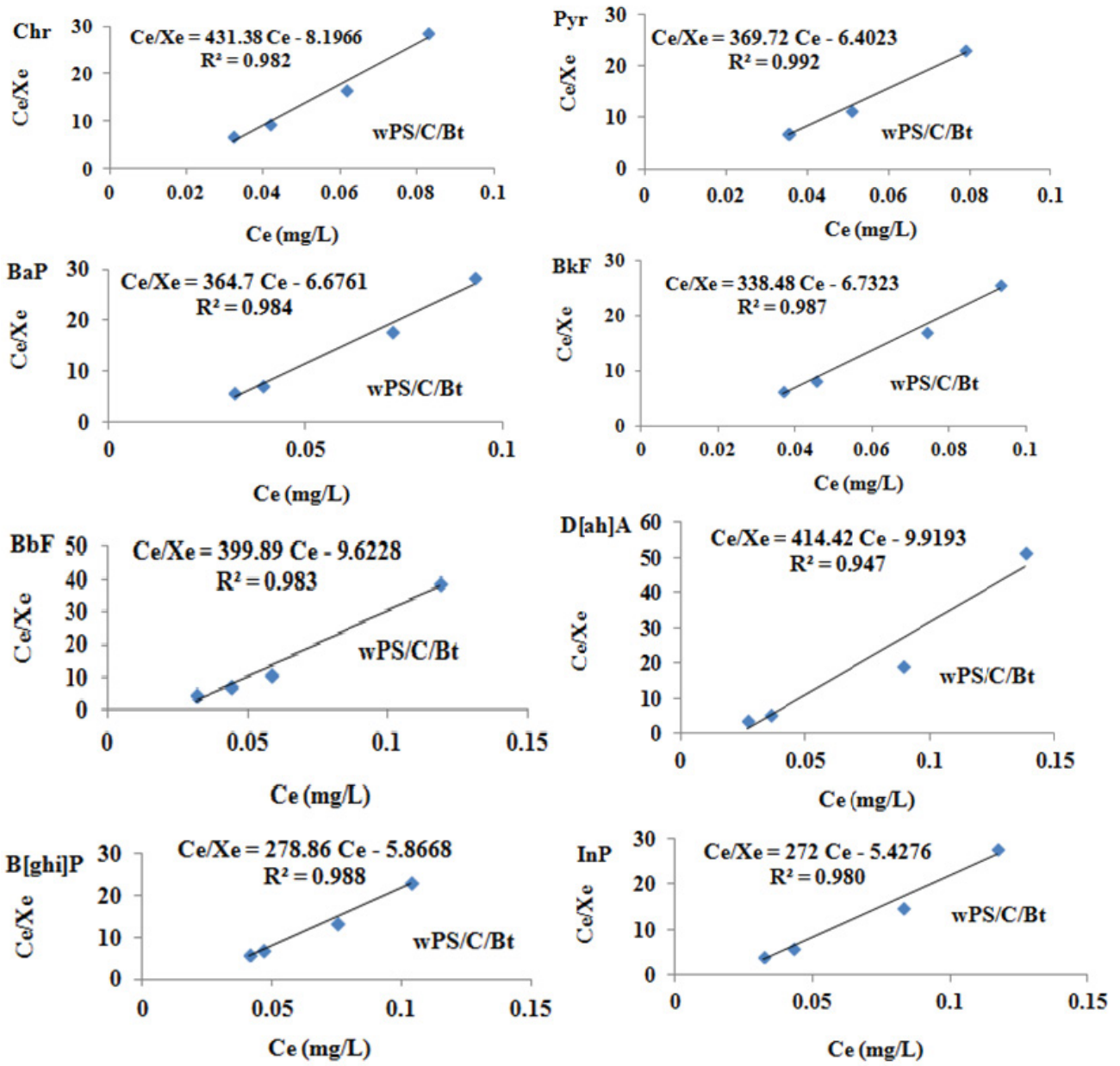Fig. S5. Plots of the Langmuir isotherms for wPS/C/Bt in batch experiment.

Chr $Ce/Xe = 431.38\ Ce - 8.1966$
$R^2 = 0.982$
wPS/C/Bt

Pyr $Ce/Xe = 369.72\ Ce - 6.4023$
$R^2 = 0.992$
wPS/C/Bt

BaP $Ce/Xe = 364.7\ Ce - 6.6761$
$R^2 = 0.984$
wPS/C/Bt

BkF $Ce/Xe = 338.48\ Ce - 6.7323$
$R^2 = 0.987$
wPS/C/Bt

BbF $Ce/Xe = 399.89\ Ce - 9.6228$
$R^2 = 0.983$
wPS/C/Bt

D[ah]A $Ce/Xe = 414.42\ Ce - 9.9193$
$R^2 = 0.947$
wPS/C/Bt

B[ghi]P $Ce/Xe = 278.86\ Ce - 5.8668$
$R^2 = 0.988$
wPS/C/Bt

InP $Ce/Xe = 272\ Ce - 5.4276$
$R^2 = 0.980$
wPS/C/Bt

Fig. S6. Plots of the Langmuir isotherms for wPS/C/Bt in batch experiment.

Nap $Ce/Xe = 209.89\, Ce - 10.326$
$R^2 = 0.961$
wPET/C/Bt

Ant $Ce/Xe = 168.77\, Ce - 3.7358$
$R^2 = 0.987$
wPET/C/Bt

Acy $Ce/Xe = 122.19\, Ce - 6.131$
$R^2 = 0.980$
wPET/C/Bt

Ace $Ce/Xe = 195\, Ce - 14.878$
$R^2 = 0.962$
wPET/C/Bt

Ph $Ce/Xe = 297.69\, Ce - 6.7762$
$R^2 = 0.979$
wPET/C/Bt

Fl $Ce/Xe = 430.46\, Ce - 4.1807$
$R^2 = 0.979$
wPET/C/Bt

Flu $Ce/Xe = 464.88\, Ce - 7.9392$
$R^2 = 0.990$
wPET/C/Bt

BaA $Ce/Xe = 443.44\, Ce - 6.2733$
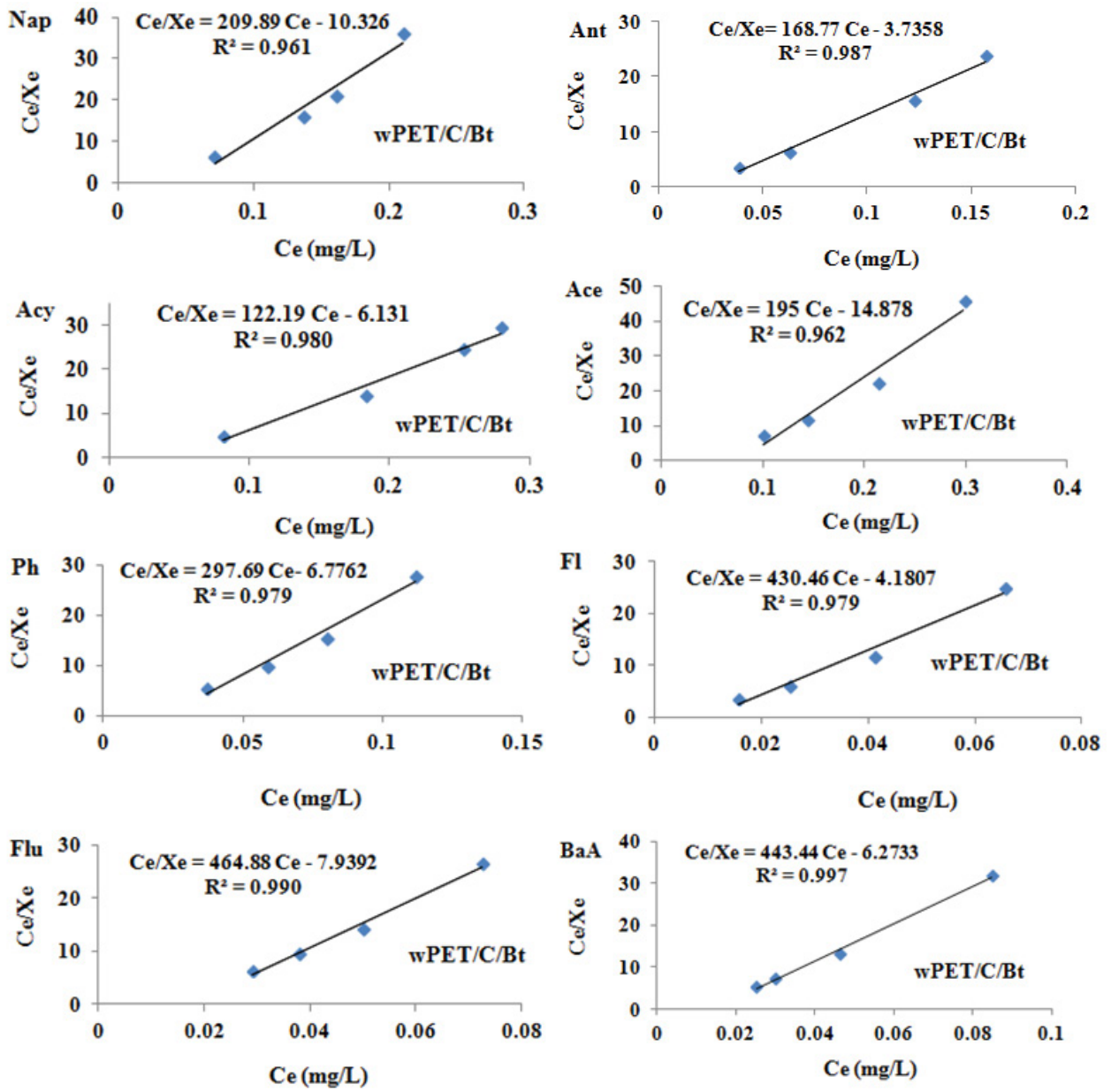$R^2 = 0.997$
wPET/C/Bt

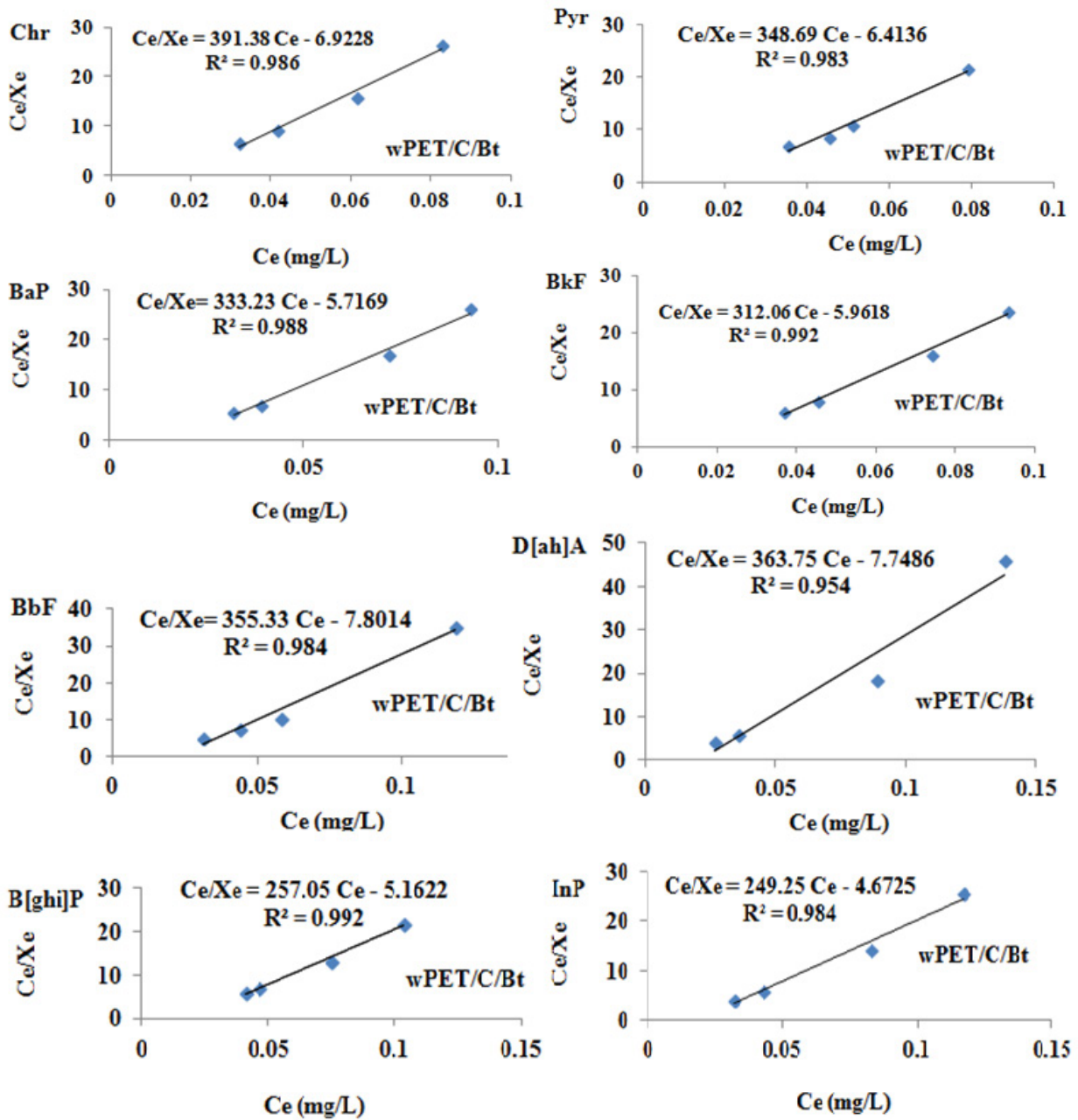Fig. S7. Plots of the Langmuir isotherms for wPET/C/Bt in batch experiment.

Fig. S8. Plots of the Langmuir isotherms for wPET/C/Bt in batch experiment.